J Therm Anal Calorim (2011) 104:613–617
DOI 10.1007/s10973-010-1074-4

# Thermogravimetric investigation of the effect of annealing conditions on the soft ferrite phase homogeneity

**A. P. Surzhikov · E. N. Lysenko · E. A. Vasendina · A. N. Sokolovskii · V. A. Vlasov · A. M. Pritulov**

Received: 23 June 2010 / Accepted: 22 September 2010 / Published online: 7 October 2010


**Abstract** In the present work, the conventional method of increasing the efficiency of solid-phase synthesis of lithium–zinc ferrites that involves multiple intermediate grinding of briquetted reaction mixtures annealed at high temperatures is compared with a new radiation-thermal (RT) method using a high-power pulsed beam of accelerated electrons for heating of reaction mixtures. An analysis of the TG(M)/DTG(M) curves recorded in a magnetic field demonstrates that the efficiency of $Li_{0.3}Zn_{0.4}Fe_{2.3}O_4$ synthesis from $Li_2CO_3$–$Fe_2O_3$–ZnO mechanical mixture at a temperature of 700 °C during 120 min is equivalent to thermal annealing at 800 °C, but with the triple annealing duration.

**Keywords** Li–Zn ferrite · Pulsed electron beam · Radiation-thermal method · Solid-state synthesis · TG(M)/DTG(M) curves

## Introduction

A low-cost simple ceramic synthesis is used for commercial production of multicomponent ferrites. This solid-phase synthesis method involves multiple high-temperature annealing of briquetted oxide and metal carbonate mixtures with intermediate grinding and mixing. All these procedures take much time, the powder can be contaminated with the grinding ball material, and the total annealing duration is long. All this can disturb the stoichiometry of the synthesized ferrite powder [1].

These disadvantages have been completely overcome in the chemical methods of synthesis capable of synthesizing the lithium ferrites at low temperatures. However, these methods have their own disadvantages, since in most cases the precursor decomposition process is accompanied by unbalanced crystallization of oxide components that could be attributed to the inhomogeneous cation distribution in the precursors [1]. Therefore, the formation of monophases requires repeated sample annealing at high temperatures. In addition, the chemical methods are complicated and ecologically not safe. Similar disadvantages are typical for other non-ceramic synthesis methods as well [2].

Thus, at present the ceramic synthesis is the basic method of commercial production of microwave ferrites. That is why the developments aimed at increasing the efficiency of ceramic synthesis are constantly underway. In particular, the efficiency of this method can be increased by the application of specific methods influencing the solid-phase systems that allow the reagents to be activated directly in the process of synthesis. Among these methods are mechanochemical [3] and microwave [4] treatment. In [5–7] it was demonstrated that the method of heating of the reaction mixture by a powerful flow of accelerated electrons is promising. The advantage of this heating method is the rapidity and low iterance of material warming up, lack of contact between the heated material and the heater, and homogeneity of material heating throughout the volume. Unlike microwave exposure, the dielectric properties of materials have no effect on electron irradiation insensitive.

It should be noted that radiation methods with the use of electron beams and gamma- and ultraviolet exposure are widely used for the modification of various systems including biological and polymeric materials [8–11].

A. P. Surzhikov · E. N. Lysenko (✉) · E. A. Vasendina · A. N. Sokolovskii · V. A. Vlasov · A. M. Pritulov
Tomsk Polytechnic University, 30, Lenin Avenue, Tomsk, Russia 634050
e-mail: lysenkoen@tpu.ru

The objective of the present work is to study the efficiency of ceramic synthesis of lithium–zinc ferrites under conditions of heating the reaction mixtures by a pulsed beam of accelerated electrons. In order to reveal the radiation effects, the lithium–zinc ferrite spinel was synthesized from the same stock reagents by the conventional scheme with intermediate grinding of briquettes and mixing of powders. The examined object was chosen due to the fact that lithium ferrite spinels alloyed with zinc provide the basis for the ferrites widely used in microwave engineering [12, 13].

The thermogravimetric method of magnetic phase monitoring in the presence of an external magnetic field was used to evaluate the efficiency of synthesis. That is, the Faraday magnetic balance method was actually used. The similar approach was used in [14] for studying some nanocrystalline and amorphous alloys.

## Experimental

We investigated the synthesis of $Li_{0.3}Zn_{0.4}Fe_{2.3}O_4$ lithium–zinc ferrites from the $Li_2CO_3$–$Fe_2O_3$–ZnO mechanical mixture. The composition was selected due to its highest saturation magnetization among the lithium-substituted ferrite spinel series [15]. Mixtures of reagents were produced by weighing the required amount of pre-dried components and then were dry-mixed in an agate mortar with 10-fold rubbing through a mesh with a 80-μm cell. The samples were compacted by single-ended cold pressing under a pressure of 200 MPa in the form of tablets with a diameter of 15 mm and thickness of 2 mm.

Thermal (T) annealing of samples was performed in a resistance furnace. Radiation-thermal (RT) annealing of samples was carried out in an ILU-6 pulse electron accelerator (Institute of Nuclear Physics of the SB RAS, Novosibirsk, Russia). The electron energy was 2.4 MeV, the beam current in the pulse was 400 mA, the pulse duration was 500 μs, and the pulse repetition frequency was 7–15 Hz. The average radiation dose was $\sim$5 kGy $s^{-1}$ at heating and $\sim$3 kGy $s^{-1}$ at isothermal annealing. The pulse radiation dose was 800 kGy $s^{-1}$. The samples were heated, and the preset temperature regime was maintained at the expense of energy of decelerated electrons without external heat sources. The duration of non-isothermal stages (heating and cooling) did not exceed 3 min. In all cases, annealing was performed in air.

The phase composition of both T and RT annealed mixtures was measured using an X-ray diffractometer (ARL X'TRA, Switzerland, with a Peltier semiconductor detector and Cu $K_\alpha$ radiation). Measurements were performed for $2\theta = 10$–$140°$ with a scan rate of $0.02° s^{-1}$. Phases were identified using the PDF-4 powder database of the International Centre for Diffraction Data (ICDD). The zinc content was refined using the lattice parameter of lithium–zinc ferrites [16]. The XRD patterns were processed by the full-profile analysis using the software *Powder Cell 2.4*.

The TG(M)/DTG(M) investigations were performed in the air atmosphere using an STA 449C Jupiter thermal analyzer (Netzsch, Germany). To control the sample magnetic state, permanent magnets ($H \sim 5$ Oe) were placed on the external side of the measuring cell. Measurements were carried out in the mode of linear cooling at a rate of 20 °C/min after the samples had been heated to 800 °C. Such measurement mode provided the initial demagnetized state of the samples.

## Results and discussion

To study the influence of the traditional homogenization method on lithium–zinc ferrite formation, four batches of the $Li_{0.3}Fe_{2.3}Zn_{0.4}O_4$ samples were prepared by annealing at 800 °C. Sample A after compacting of the initial reaction mixture was annealed during 120 min. Sample B was annealed during 240 min. Samples C and D were annealed during 360 min. The preparation of samples B and C involved intermediate powder grinding and mixing. These procedures were performed every 120 min during annealing and were followed by three procedures including sample trituration using an agate mortar and pestle, 10-fold rubbing through a mesh, and repeated pressing into tablets. Samples A and D were annealed without intermediate mixing and differed only in the annealing time.

Figure 1 shows fragments of the X-ray powder diffraction patterns for samples A, C, and D that demonstrate the influence of the annealing duration and 2-fold intermediate mixing on the phase homogeneity of the powder. For annealing during 120 min (Fig. 1a), the phase inhomogeneity of sample A is manifested through peak broadening, splitting of reflections, and presence of the (210) and (211) superstructure reflection peaks corresponding to the zinc lightly doped pentaferrite phase. The triple increase in the annealing duration without intermediate grinding and mixing (Fig. 1b) significantly reduces the peak broadening and splitting of reflections. However, the superstructure reflections of pentaferrite phase ($LiFe_5O_8$) are still present on the diffraction pattern. And only double intermediate grinding and mixing of samples yields the simplest diffraction patterns (sample C in Fig. 1c). In the X-ray diffraction pattern shown in Fig. 1c, only the narrowest reflections of the spinel phase without superstructure reflections and splitting can be seen. This demonstrates the maximum degree of homogenization achieved for the synthesized powder.

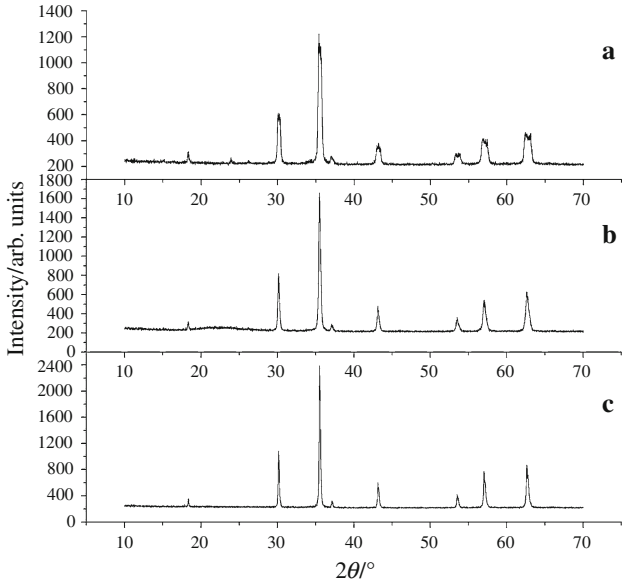


**Fig. 1** XRD patterns of samples A (**a**), D (**b**), and C (**c**)

**Table 1** Influence of the annealing duration ($t$) and multiplicity of intermediate mixing ($n$) on the ferrite powder phase composition

| Sample | $n$ ($t$/min) | Phases | C/mass% |
|---|---|---|---|
| A | 0 (120) | $Li_{0.1}Zn_{0.8}Fe_{2.1}O_4$ | 44 |
| | | $Li_{0.35}Zn_{0.3}Fe_{2.35}O_4$ | 35 |
| | | $Li_{0.48}Zn_{0.04}Fe_{2.45}O_4$ | 21 |
| B | 1 (120 + 120) | $Li_{0.205}Zn_{0.59}Fe_{2.205}O_4$ | 8 |
| | | $Li_{0.315}Zn_{0.37}Fe_{2.315}O_4$ | 75 |
| | | $Li_{0.48}Zn_{0.04}Fe_{2.48}O_4$ | 17 |
| C | 2 (120 + 120 + 120) | $Li_{0.2}Zn_{0.6}Fe_{2.2}O_4$ | 0 |
| | | $Li_{0.315}Zn_{0.37}Fe_{2.315}O_4$ | 93 |
| | | $Li_{0.48}Zn_{0.04}Fe_{2.48}O_4$ | 7 |
| D | 0 (360) | $Li_{0.225}Zn_{0.55}Fe_{2.225}O_4$ | 28 |
| | | $Li_{0.34}Zn_{0.32}Fe_{2.34}O_4$ | 47 |
| | | $Li_{0.485}Zn_{0.03}Fe_{2.485}O_4$ | 25 |

The results of powder phase analysis at different stages of thermal synthesis at a temperature of 800 °C are shown in Table 1.

The table demonstrates that the synthesis during 360 min with double intermediate mixing leads to the formation of virtually single-phase homogeneous product, whereas in the absence of mixing, the intermediate phase content increases sharply.

Figure 2 shows the DTG(M) curves that demonstrate the presence of two mass transitions in the magnetic field. Here, the mass jump at ca. 630 °C is explained by the transition through the Curie temperature in the lithium pentaferrite and the smeared low-temperature transition most likely caused by the formation of lithium–zinc ferrite phases.

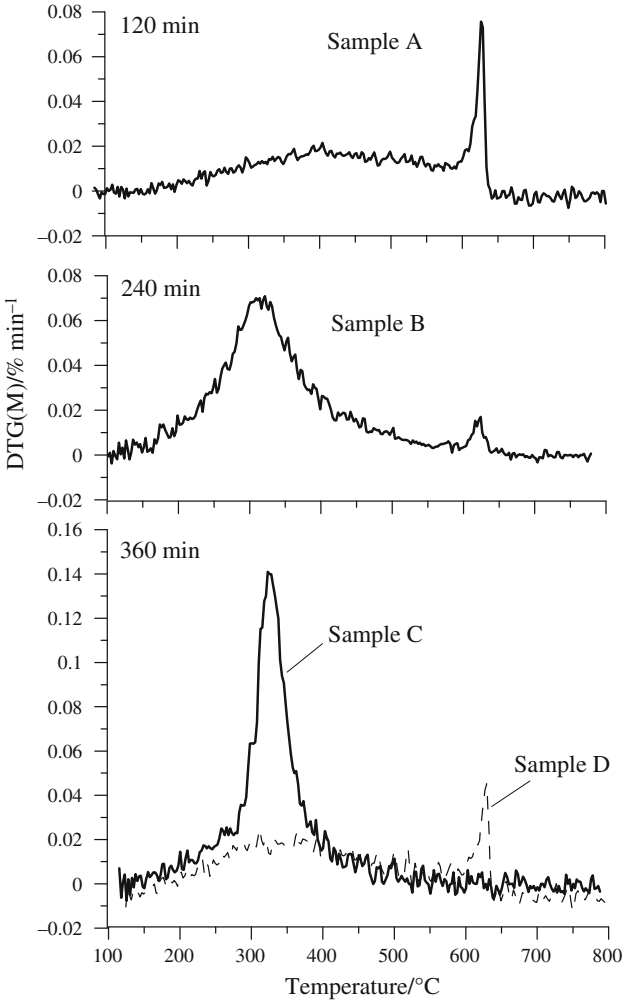


**Fig. 2** DTG(M) curves of $Li_{0.3}Zn_{0.4}Fe_{2.3}O_4$ thermally synthesized at 800 °C with different annealing durations and grinding and mixing frequencies

For sample A, the phase inhomogeneity is manifested through a strongly smeared low-temperature magnetic transition in the Li–Zn ferrite phase, shift of its maximum toward higher temperatures, and the presence of the high-temperature transition of the pentaferrite phase through the Curie temperature (the peak at ca. 630 °C). The presence of $LiFe_5O_8$ is indicative not only of the extremely low material homogeneity, but also of the incompleteness of the synthesis reaction itself. The increase of the annealing duration and the incorporation of intermediate powder mixing decrease the transition width in the lithium–zinc ferrite phase and reduce the content of the pentaferrite phase (sample B) to its disappearance (sample C).

The importance of mixing follows from a comparison of the DTG(M) curves of samples C and D having the same annealing durations (360 min). The absence of intermediate mixing of sample D results in a wide transition in the lithium–zinc ferrite phase, which is indicative of much higher spread of the zinc content in these phases.

The DTG(M) curves measured for the reference $Li_{0.5(1-x)}Zn_xFe_{2.5-0.5x}O_4$ samples with controllable zinc content $x_{Zn}$ made it possible to obtain the concentration dependence of the magnetic transition temperature. The samples were prepared by thermal synthesis at 800 °C during 360 min with intermediate grindings and mixing every 120 min during annealing. Figure 3 shows the DTG(M) curves for the specified samples. The position of maximum in every curve corresponds to the Curie temperature of the composition with $x_{Zn} = 0$, 0.1, 0.2, 0.4, and 0.6. The inset figure shows the concentration dependence of the Curie temperature that decreases linearly, which is typical for lithium–zinc ferrite spinels [4]. It can also be seen that the width of the magnetic transition (the DTG(M) peak width) increases with the zinc content.

The irradiation-induced effect of enhancement of the ferrite powder homogenization process at heating of reaction mixtures by accelerated electron beams is proved by means of a comparison of the DTG(M) curves for the samples synthesized under conditions of T and RT annealing at a temperature of 700 °C during 120 min. These curves are shown in Fig. 4.

From Fig. 4, it can be seen that a decrease in the thermal annealing temperature by 100 °C leads to a more smeared Li–Zn ferrite phases and a relative increase of the lithium pentaferrite content compared to the data of Fig. 3 (sample A). Vice versa, heating by the electron beam, despite the annealing temperature decrease by 100 °C, yields the result equivalent to the data of Fig. 3 for sample D.

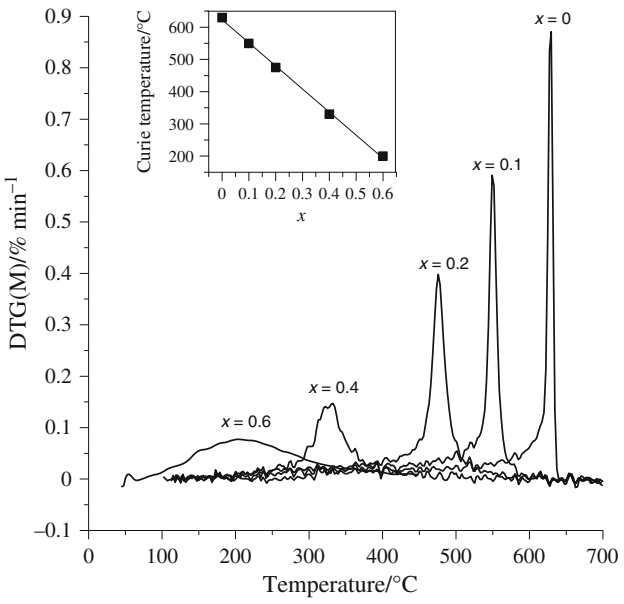


**Fig. 3** DTG(M) curves of $Li_{0.5(1-x)}Zn_xFe_{2.5-0.5x}O_4$ with $x_{Zn} = 0$, 0.1, 0.2, 0.4, and 0.6 thermally synthesized at 800 °C during 360 min with intermediate grinding and mixing

The diffraction patterns for the RT samples shown in Fig. 5b comprise only narrow reflections of the spinel phase and no visible signs of splitting.

The phase composition of T and RT samples annealed at 700 °C (without intermediate mixing) is shown in Table 2. It can be seen that in the RT mode, the ferritization degree of the final product is more than doubled compared to the result of thermal annealing. No phases of the initial components are present. Whereas the $LiFe_5O_8$ phase dominates as an intermediate phase in the T mode of synthesis, the lithium–zinc ferrite with reduced zinc content $Li_{0.49}Zn_{0.02}Fe_{2.49}O_4$ whose concentration is almost halved dominates after the RT synthesis.

From the data of Table 2, it follows that the reaction of lithium–zinc ferrite formation is incomplete for both T and RT modes. However, a comparison with Table 1

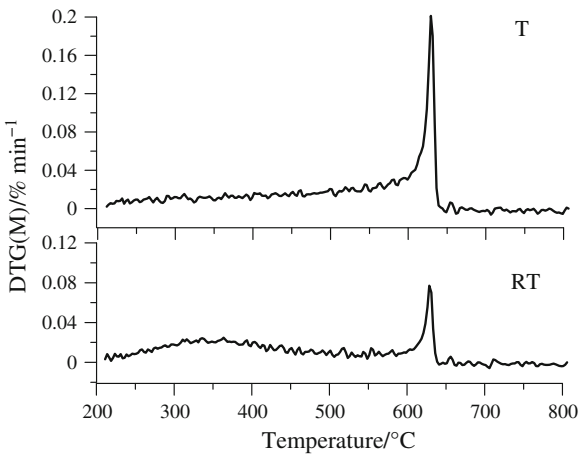


**Fig. 4** DTG(M) curves of $Li_{0.3}Zn_{0.4}Fe_{2.3}O_4$ synthesized under conditions of T and RT annealing at 700 °C during 120 min

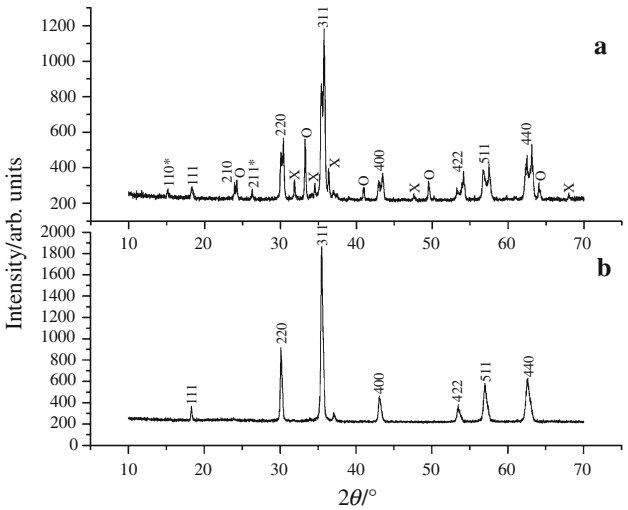


**Fig. 5** XRD patterns of the samples synthesized at 700 °C during 120 min using T (**a**) and RT (**b**) modes

**Table 2** Phase composition of T and RT samples synthesized in regime 700 °C during 120 min

| Mode | Phases | C/mass% |
|---|---|---|
| T | $Li_{0.5}Fe_{2.5}O_4$ | 27.6 |
| | $Li_{0.375}Zn_{0.25}$ $Fe_{2.375}O_4$ | 22.7 |
| | $Li_{0.1}Zn_{0.8}Fe_{2.1}O_4$ | 26.1 |
| | $Fe_2O_3$ | 17.9 |
| | $Li_{0.086}Zn_{0.914}O_{0.957}$ | 5.7 |
| RT | $Li_{0.49}Zn_{0.02}Fe_{2.49}O_4$ | 14.4 |
| | $Li_{0.31}Zn_{0.38}Fe_{2.31}O_4$ | 79.9 |
| | $Li_{0.205}Zn_{0.59}Fe_{2.205}O_4$ | 5.7 |
| | $Fe_2O_3$ | 0 |
| | $Li_{0.086}Zn_{0.914}O_{0.957}$ | 0 |

demonstrates almost equivalent results of the reaction mixture synthesis by electron beam heating during 120 min and by heating in the resistance furnace during 240 min with mixing. Herewith, the RT synthesis temperature was by 100 °C lower than the T synthesis temperature.

Thus, the efficiency of the RT synthesis at a temperature of 700 °C during 120 min without intermediate grinding and mixing is equivalent to that of the thermal synthesis at 800 °C but with twice as long duration.

## Conclusions

Based on the foregoing, we can conclude that for the multicomponent heterogeneous system of the powder reagent mixture, the formation of the final product occurs through the continuous series of the $Li_{0.5(1-x)}Zn_x$ $Fe_{2.5-0.5x}O_4$ spinel phases, where $x$ changes from 0 to 1, due to the topological character of the solid-phase synthesis reaction. This circumstance broadens the Li–Zn ferrite magnetic phase transition at the Curie temperature. The transition width is determined by the conditions and duration of annealing.

The use of intermediate grinding of briquetted mixtures with powder mixing as well as mixture heating upon exposure to electron beams lead to intensification of lithium–zinc ferrite solid-phase synthesis and enhancement of the final product homogeneity.

High efficiency of complex multicomponent oxide solid-state synthesis in case of reaction mixture annealing by high-power electron beams is most likely due to the high rate of diffusion-controlled lithium carbonate and zinc oxide dissolution.

## References


1. Ahniyaz A, Fujiwara T, Song S-W, Yoshimura M. Low temperature preparation of $\beta$-$LiFe_5O_8$ fine particles by hydrothermal ball milling. J Solid State Ionics. 2002;151:419–23.
2. Cook W, Manley M. Raman characterization of $\alpha$- and $\beta$-$LiFe_5O_8$ prepared through a solid-state reaction pathway. J Solid State Chem. 2010;183:322–6.
3. Berbennia V, Marinia A, Matteazzib P, Riccerib R, Welhamc NJ. Solid-state formation of lithium ferrites from mechanically activated $Li_2CO_3$–$Fe_2O_3$ mixtures. J Eur Ceram Soc. 2003;23:527–36.
4. Yasuoka M, Nishimura Y, Nagaoka T, Watari K. Influence of different methods of controlling microwave sintering. J Therm Anal Calorim. 2006;83:407–10.
5. Lyakhov NZ, Boldyrev VV, Voronin AP, Gribkov OS, Bochkarev LG, Rusakov SV, Auslender VL. Electron beam stimulated chemical reaction in solids. J Therm Anal Calorim. 1995;43:21–31.
6. Surzhikov AP, Pritulov AM, Ivanov YF, Shabardin RS, Usmanov RU. Electron-microscopic study of morphology and phase composition of lithium-titanium ferrites. J Russ Phys. 2001;44:420–3.
7. Surzhikov AP, Pritulov AM, Lysenko EN, Sokolovskiy AN, Vlasov VA, Vasendina EA. Calorimetric investigation of radiation-thermal synthesized lithium pentaferrite. J Therm Anal Calorim. 2010;101:11–3.
8. Nemtanu MR, Brasoveanu M, Meltzer V, Pincu E, Oproiu C. Thermal analysis of some phytotherapeutic products irradiated with electron beam. J Therm Anal Calorim. 2009;97:309–13.
9. Ciesla K, Vansant EF. Physico-chemical changes taking place in gamma irradiated bovine globulins studied by thermal analysis. J Therm Anal Calorim. 2010;99:315–24.
10. Vychopnova J, Cermak R, Obadal M, Verney V, Commereuc S. Effect of $\beta$-nucleation on crystallization of photodegraded polypropylene. J Therm Anal Calorim. 2009;95:215–20.
11. Sen M, Çopuroglu M. Influence of gamma irradiation on the ageing characteristics of poly(ethylene-co-vinil acetate) and poly(ethylene-co-vinyl acetate) carbon black mixture. J Therm Anal Calorim. 2006;86:223–7.
12. Baba PD, Argentina GM, Courtney WE, Dionne GF, Temme DH. Fabrication and properties of microwave lithium ferrites. IEEE Trans Magn. 1972;8:83–94.
13. Jiang XN, Lan ZW, Yu Z, Liu PY, Chen DZ, Liu CY. Sintering characteristics of LiZn ferrites fabricated by a sol–gel process. J Magn Magn Mater. 2009;321:52–5.
14. Lin DM, Wang HS, Lin ML, Lin MH, Wu YC. TG(M) and DTG(M) techniques and some of their applications on material study. J Therm Anal Calorim. 1999;58:347–53.
15. Gorter EW. Saturation magnetization and crystal chemistry of ferrimagnetic oxides. J Philips Res Rep. 1954;9:295.
16. Shiliakov SM, Maltsev VI, Ivolga VV, Naiden EP. Atomic structure of lithium–zinc–iron spinels. Izv Vyss Uchebnykh Zaved Moskva Ser Fiz. 1977;1:111–6.